Molecular Structure in Solution: An ab Initio Vibrational Spectroscopy Study of Phenyloxirane

C. S. Ashvar,† F. J. Devlin, and P. J. Stephens*

Department of Chemistry, University of Southern California, Los Angeles, California 90089-0482

Received September 15, 1998. Revised Manuscript Received December 28, 1998

Abstract: We report a study of the structure of phenyloxirane (**1**) in solution using ab initio vibrational spectroscopy. Vibrational unpolarized absorption and circular dichroism spectra of **1** in CCl_4 and CS_2 solutions are measured. Harmonic potential energy surfaces and, thence, harmonic frequencies, dipole strengths, and rotational strengths of the fundamental modes of **1** are calculated ab initio using Hartree−Fock/self-consistent field (HF/SCF), MP2 and density functional theory (DFT) methods. DFT/B3LYP/TZ2P vibrational spectra are in excellent agreement with experimental spectra; alternative combinations of functional and basis set yield less good agreement. HF/SCF and MP2 calculations yield spectra in even poorer agreement with experiment. The DFT/B3LYP/TZ2P equilibrium structure is therefore the most accurate. The plane of the phenyl ring is tilted from perpendicular to the plane of the oxirane ring by 14.5°. The direction of tilt brings a phenyl ortho H closer to the oxirane O. The direction and magnitude of tilt can be understood in terms of the competing forces of pseudoconjugation, C−H···O hydrogen bonding and H···H van der Waals repulsion. The DFT/B3LYP/TZ2P dipole moment agrees with experiment within experimental error.

Introduction

We report a study of the molecular structure of phenyloxirane (**1**) in solution using ab initio vibrational spectroscopy. We take advantage of recent developments in ab initio density functional theory (DFT)[1] and vibrational circular dichroism (VCD) spectroscopy.[2]

Neither X-ray diffraction techniques, so widely used to study molecular structure in the crystalline solid state, nor microwave spectroscopic, infrared spectroscopic, or electron diffraction techniques, used to study molecular structure in the gas phase, are applicable to the determination of molecular structure in condensed-phase amorphous solutions. Of the techniques which are applicable to the study of solution structure, vibrational spectroscopy is one of the most heavily used. There are multiple vibrational spectroscopic techniques. Infrared absorption using unpolarized radiation and Raman scattering using linearly polarized radiation are the most commonly employed. The techniques of VCD[2] and Raman optical activity (ROA)[3] are also available when the molecule is chiral.

Vibrational spectra and molecular structure are interconnected via the molecular potential energy surface (PES). The molecular structure is the geometry at equilibrium: the PES minimum. Vibrational frequencies, coordinates, and intensities reflect the PES in the neighborhood of the minimum. It follows that a PES which accurately predicts vibrational spectra simultaneously and equally accurately predicts the equilibrium geometry. Ab initio quantum chemistry is increasingly used in predicting vibrational spectra, as a result of the continuing increase in both accuracy and efficiency of ab initio methods. Recently, developments in DFT have enormously enhanced the utility of this specific ab initio methodology, making it currently the method of choice for many molecules, especially those of larger size. These developments include analytical derivative techniques for harmonic vibrational frequencies, unpolarized absorption ("IR") intensities and VCD intensities,[4] "hybrid" density functionals,[5] and more efficient computational algorithms. Older methodologies, such as the Hartree−Fock/self-consistent field (HF/SCF) and second-order Møller−Plesset (MP2) approaches,[6] are less accurate and/or computationally efficient and are of decreasing utility.

The present study focuses on the solution structure of the chiral molecule phenyloxirane (**1**) (Figure 1). IR unpolarized absorption and VCD spectra of CCl_4 and CS_2 solutions are measured. Calculations of the harmonic PES and, thence, of the harmonic frequencies, absorption intensities, and VCD intensities of the fundamentals of **1** are carried out using the DFT, HF/SCF, and MP2 methodologies; in the case of DFT, two functionals and two basis sets are used. Comparison to the experimental spectra enables the accuracies of the predicted vibrational spectra and, in turn, of the predicted equilibrium geometries to be assessed. At the same time, the vibrational spectra of **1** are assigned.

Prior experimental studies of the structure of **1** are limited. There have been no studies of **1** using either diffraction or spectroscopic methods. An X-ray structure of *p*-nitrophenyloxirane (**2**) has been reported.[7] The conformation of **2** is "tilted", i.e., the phenyl ring is between the "bisected" and the "perpendicular" conformations (Figure 2). The direction of tilt from

* To whom correspondence should be addressed.
† Present address: Nexstar Pharmaceuticals, 650 Cliffside Dr., San Dimas, CA 91773.

(1) *Chemical Applications of Density Functional Theory*; Laird, B. B., Ross, R. B., Ziegler, T., Eds.; ACS Symposium Series 629, American Chemical Society: Washington, DC, 1996.
(2) Stephens, P. J.; Lowe, M. A. *Annu. Rev. Phys. Chem.* **1985**, *36*, 213.
(3) Nafie, L. A. *Annu. Rev. Phys. Chem.* **1997**, *48*, 357.
(4) (a) Johnson, B. G.; Frisch, M. J. *Chem. Phys. Lett.* **1993**, *216*, 133. (b) Johnson, B. G.; Frisch, M. J. *J. Chem. Phys.* **1994**, *100*, 7429. (c) Cheeseman, J. R.; Frisch, M. J.; Devlin, F. J.; Stephens, P. J. *Chem. Phys. Lett.* **1996**, *252*, 211.
(5) Becke, A. D. *J. Chem. Phys.* **1993**, *98*, 1372, 5648.
(6) Hehre, W. J.; Radom, L.; Schleyer, P. R.; Pople, J. A. *Ab Initio Molecular Orbital Theory;* Wiley: New York, 1986.
(7) Williams, D. J.; Crotti, P.; Macchia, B.; Macchia, F. *Tetrahedron* **1975**, *31*, 993.

10.1021/ja983302y CCC: $18.00
Published on Web 03/11/1999

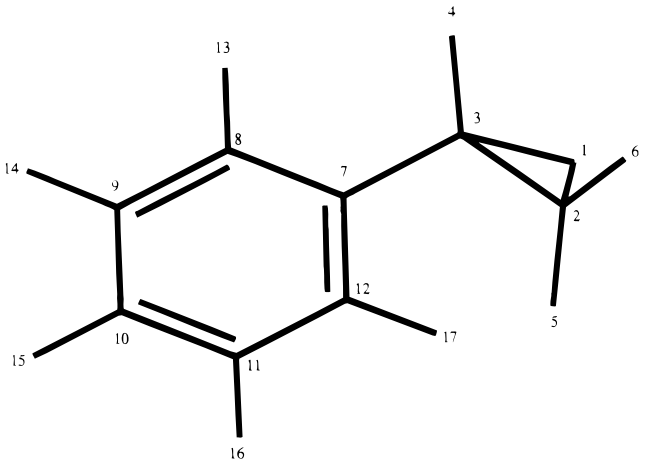

Figure 1. Phenyloxirane, **1**. Atom numbering used in the text and in Tables 1 and 4 is shown.

bisected brings an ortho C−H group closer to the oxirane O. The angle between the planes of the oxirane and phenyl rings is 80.2°, i.e., the tilt angle of the phenyl ring from bisected is 9.8°. Measurement of the dipole moments of **1** and a number of derivatives led to the conclusion that the phenyl ring exhibits free rotation about the bond to the oxirane ring.[9] Subsequent study of the electro-optic Kerr effect of **1** and several derivatives led to the opposite conclusion, and determined the structure of **1** to be tilted with a tilt angle of $18 \pm 9°$ (although the presence of a second conformation rotated by ∼90° could not be ruled out).[10] Prior theoretical studies of **1** are also limited. Semiempirical CNDO/2 calculations of the variation in energy with rotation of the phenyl group found (1) a single minimum, corresponding to a tilted structure with a tilt angle of ∼35°[11] or ∼30°;[12] (2) a maximum at a tilt angle differing by ∼70°[11] or ∼90°;[12] (3) a barrier height of 3.54[11] or 3.15[12] kcal/mole. There do not appear to have been prior ab initio calculations of the structure and/or vibrational spectra of **1**.

Methods

Absorption spectra of **1** were measured at 1 cm^{-1} resolution using Nicolet MX-1 and Bomem/Biotools Chiral*IR*[13] FTIR spectrometers. Absorption and VCD spectra of **1** were measured at 4 cm^{-1} resolution using the Chiral*IR* instrument. Data collection for each VCD spectrum was 2 h. CCl_4 and CS_2 solutions were studied. Cells were fixed path (ICl) with KBr windows. VCD intensities were calibrated using reference VCD data for α-pinene.[14]

S-(−)-, R-(+)- and (±)-**1** were obtained from Aldrich and used without further purification. Specified chemical purities were: S-(−), 98%; R-(+), 98%; (±), 97%. Specified enantiomeric purities and specific rotations were S-(−), 97%, $[\alpha]^{20}_D = -33°$ (neat); R−(+), 97%, $[\alpha]^{20}_D = +33°$ (neat).

All ab initio calculations were carried out using the GAUSSIAN program[15] as described previously.[16] All calculations used analytical derivative techniques.[4] The basis sets were [3s2p1d/2s]/6-31G*[6] (151 basis functions for **1**) and [5s4p2d/3s2p]/TZ2P[17] (333 basis functions for **1**). DFT calculations were carried out using the hybrid functionals B3LYP and B3PW91.[5,18] HF/SCF and DFT atomic axial tensors (AATs) were calculated using gauge-invariant atomic orbitals (GIAOs).[4c] MP2 GIAO AATs are not available; accordingly VCD intensities were not calculated at the MP2 level.

Experimental spectra were fit using Lorentzian band shapes to obtain frequencies, dipole strengths, and rotational strengths as described previously.[16b,c] The VCD spectrum was fit with frequencies and bandwidths constrained to the values obtained in fitting the Chiral*IR* 4 cm^{-1} resolution absorption spectrum. Absorption and VCD spectra were also obtained from calculated frequencies, dipole strengths, and rotational strengths using Lorentzian band shapes of constant width.

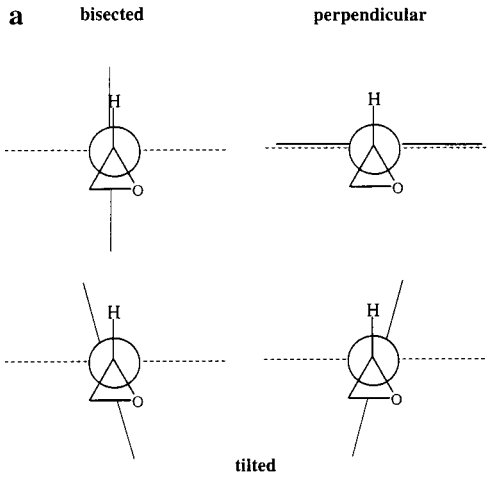

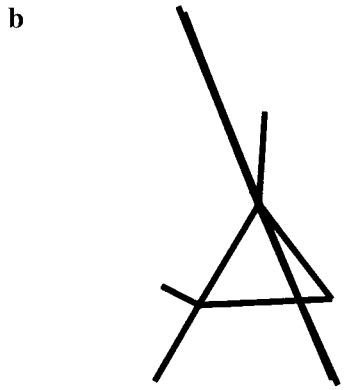

Figure 2. (a) Conformations of **1**. Nomenclature for "bisected" and "perpendicular" conformations follows Allen[8]. (b) The DFT/B3LYP/TZ2P structure of **1**, viewed along the C3−C7 bond, showing the "tilted" conformation.

Results

DFT/B3LYP/TZ2P Calculations. Geometry optimization at the TZ2P basis set level using the B3LYP functional leads to the structural parameters given in Table 1. The conformation is tilted (Figure 2). The angle between the plane of the oxirane ring and the plane defined by the atoms C7, C8, and C12 of the phenyl ring is 75.5° i.e., the tilt angle is 14.5°. [Note that, since the phenyl ring in **1** is not exactly planar, the definition

(8) Allen, F. H. *Acta Crystallogr.* **1980**, *B36*, 81.
(9) Sorriso, S.; Battistini, C.; Macchia, B.; Macchia, F. *Z. Naturforsch.* **1977**, *32b*, 1467.
(10) Aroney, M. J.; Calderbank, K. E.; Stootman, H. J. *J. Mol. Struct.* **1983**, *99*, 259.
(11) Lazzeretti, P.; Moretti, I.; Taddei, F.; Torre, G. *Org. Magn. Reson.* **1973**, *5*, 385.
(12) Sorriso, S.; Stefani, F.; Semprini, E.; Flamini, A. *J. Chem. Soc., Perkin Trans. 2* **1976**, *4*, 374.
(13) Bomem, Inc., Quebec, Canada; BioTools, Elmhurst, Illinois.
(14) Professor L. A. Nafie, Syracuse University, private communication, 1997.
(15) Frisch, M. J. et al., GAUSSIAN 94; GAUSSIAN 95 (Development Version), Gaussian Inc.: Pittsburgh, PA.
(16) (a) Stephens, P. J.; Ashvar, C. S.; Devlin, F. J.; Cheeseman, J. R.; Frisch, M. J. *Mol. Phys.* **1996**, *89*, 579. (b) Devlin, F. J.; Stephens, P. J.; Cheeseman, J. R.; Frisch, M. J. *J. Phys. Chem. A* **1997**, *101*, 6322. (c) Devlin, F. J.; Stephens, P. J.; Cheeseman, J. R.; Frisch, M. J. *J. Phys. Chem. A* **1997**, *101*, 9912.
(17) Stephens, P. J.; Jalkanen, K. J.; Amos, R. D.; Lazzeretti, P.; Zanasi, R. *J. Phys. Chem.* **1990**, *94*, 1811.
(18) Stephens, P. J.; Devlin, F. J.; Chabalowski, C. F.; Frisch, M. J. *J. Phys. Chem.* **1994**, *98*, 11623.

Table 1. Structural Parameters for Phenyloxirane (**1**) and *p*-Nitrophenyloxirane (**2**)[a,b]

	1						**2**	
	DFT				MP2	HF/SCF	EXPT[e]	DFT
	B3LYP/ TZ2P	B3PW91/ TZ2P[d]	B3LYP/ 6-31G*[d]	B3PW91/ 6-31G*[d]	6-31G*[d]	6-31G*[d]		B3LYP/TZ2P
				Bond Lengths				
1,2	1.430 (−1)[c]	−8 (−1)[c]	0 (0)[c]	−8 (−1)[c]	9 (0)[c]	−27 (1)[c]	1.430 (−2−4)[f]	1.429 (−1)[g]
1,3	1.433 (3)	−8 (3)	2 (5)	−6 (4)	11 (5)	−32 (0)	1.434 (0−6)	1.430 (−4)
2,3	1.474(9)	−4 (9)	4 (9)	0 (9)	−2 (8)	−15 (6)	1.448 (−22−(−14))	1.475 (27)
3,7	1.488	−3	4	1	−2	7	1.487	1.487 (0)
7,8	1.395 (4)	−2 (4)	5 (4)	3 (3)	5 (3)	−6 (3)	1.389 (−1)	1.397 (8)
8,9	1.390 (−1)	−2 (−2)	5 (−2)	3 (−2)	5 (−2)	−5 (−1)	1.379 (−11)	1.386 (7)
9,10	1.390 (−1)	−2 (−1)	6 (0)	4 (−1)	7 (0)	−4 (−1)	1.377 (−13)	1.388 (11)
10,11	1.391 (0)	−2 (0)	6 (0)	4 (0)	6 (0)	−5 (−1)	1.377 (−13)	1.389 (12)
11,12	1.389 (−2)	−2 (−2)	5 (−2)	3 (−2)	6 (−2)	−4 (−1)	1.383 (−7)	1.386 (3)
7,12	1.395 (4)	−2 (3)	5 (4)	3 (3)	5 (3)	−6 (3)	1.389 (−1)	1.396 (7)
				Bond Angles				
2,1,3	62.0 (0.4)	0.2 (0.4)	0.1 (0.3)	0.3 (0.3)	−0.6 (0.2)	0.7 (0.3)	60.7 (−0.9)	62.1 (1.4)
1,2,3	59.1 (−0.1)	−0.1 (−0.1)	0 (0.0)	−0.1 (0)	0.3 (0)	−0.5 (−0.2)	59.8	59.0 (−0.8)
1,3,2	58.9 (−0.3)	−0.1 (−0.3)	−0.1 (−0.3)	−0.2 (−0.3)	0.2 (−0.3)	−0.2 (−0.1)	59.5	58.9 (−0.6)
1,3,7	117.8	0	−0.1	−0.2	−1.0	−0.2	116.5	117.6 (1.1)
2,3,7	122.5	−0.3	−0.2	−0.5	−1.2	−0.1	121.7	122.0 (0.3)
3,7,8	119.5	0.1	0.3	0.4	0.3	0.1		119.5
3,7,12	121.3	−0.1	−0.3	−0.4	−0.8	−0.1 (1.2)		121.1
7,8,9	120.6 (0.6)	−0.1 (0.5)	−0.1 (0.5)	−0.2 (0.4)	−0.4 (0.2)	−0.1 (0.5)	120.6	120.8 (0.2)
8,9,10	120.1 (0.1)	0 (0.1)	0 (0.1)	0 (0.1)	0 (0.1)	−0.1 (0)	118.5 (−1.5)	118.6 (0.1)
9,10,11	119.6 (−0.4)	0 (−0.4)	0.1 (−0.3)	0.1 (−0.3)	0.2 (−0.2)	0.1 (−0.3)		121.8
10,11,12	120.3 (0.3)	0 (0.3)	0 (0.3)	0 (0.3)	0 (0.3)	0 (0.3)	118.4 (−1.6)	118.9 (0.5)
11,12,7	120.3 (0.3)	0 (0.3)	0 (0.3)	0 (0.3)	−0.3 (0)	−0.1 (0.2)	120.5 (0.5)	120.5 (0)
8,7,12	119.1 (−0.9)	0.1 (−0.8)	0.1 (−0.8)	0.2 (−0.7)	0.6 (−0.3)	0.1 (−0.8)	119.6 (−0.4)	119.4 (−0.2)
				Dihedral Angles[h]				
1,2,3,7	105.2	0.1	0.2	0.1	0.6	0.4		105.1
1,3,7,8	163.9	0.9	1.0	2.4	4.5	7.2		165.8
1,3,7,12	16.4	0.8	0.7	2.1	3.2	6.9	24.0	14.5 (−9.5)
2,3,7,8	126.9	0.6	0.7	1.8	3.9	6.7		125.4
2,3,7,12	52.7	0.6	0.5	1.6	2.6	6.5	45.0	54.3 (9.3)
3,7,8,9	178.7	0	0.2	0.2	0.6	0.1		178.7
3,7,12,11	178.9	0	0.2	0.2	0.8	0		178.9
7,8,9,10	0.5 (0.5)	0 (0.5)	0 (0.5)	0.1 (0.4)	0.5 (0.0)	0.1 (0.4)		0.5
8,9,10,11	0.2 (0.2)	0 (0.2)	0 (0.2)	0 (0.2)	0.2 (0.4)	0.1 (0.1)		0.3
9,10,11,12	0.4 (0.4)	0 (0.4)	0 (0.4)	0 (0.4)	0.1 (0.5)	0.1 (0.3)		0.5
10,11,12,7	0.0 (0.0)	0 (0.0)	0.1 (0.1)	0.1 (0.1)	0.2 (0.2)	0.1 (0.1)		0.1
11,12,7,8	0.7 (0.7)	0 (0.7)	0 (0.7)	0 (0.7)	0.5 (0.2)	0.2 (0.5)		0.8
12,7,8,9	0.9 (0.9)	0 (0.9)	0 (0.9)	0 (0.9)	0.6 (0.3)	0.2 (0.7)		1.0
8,7,3,4 (D)	25.6	0.4	0.7	1.8	4.9	7.4	20.0	27.0 (7.0)
				Tilt Angles[i]				
	14.5	0.1	0.2	0.6	0.4	3.5	9.8	15.1

[a] Bond lengths in Å, bond and dihedral angles in degrees. Atom numbering as in Figure 1. [b] Parameters involving H atoms are omitted; complete tabulations of structural parameters for **1** are given in ref 19. [c] Numbers in parentheses are differences (in 10^{-3} Å for bond lengths and degrees for angles) from corresponding parameters in oxirane and benzene (Table 2). [d] Differences (in 10^{-3} Å for bond lengths and degrees for angles) from corresponding DFT/B3LYP/TZ2P parameters. [e] Values from X-ray structure of *p*-nitrophenyloxirane (**2**).[7] [f] Numbers in parentheses are differences (in 10^{-3} Å for bond lengths and degrees for angles) from corresponding experimental parameters for oxirane and benzene (Table 2). [g] Numbers in parentheses are differences (in 10^{-3} Å for bond lengths and degrees for angles) from experimental parameters. [h] Signs are omitted. [i] The tilt angle is the difference from 90° of the angle between the O1C2C3 and C8C7C12 planes.

of the tilt angle is not unique; in this work we define the plane of the phenyl ring as the C7−C8−C12 plane.] The dihedral angle of atoms C8−C7−C3−H4 (henceforth D), is 25.6°. The direction of tilt is such as to bring a phenyl ortho-H (H17) closer to the oxirane O than in the bisected conformation.

The geometries of the oxirane and phenyl rings are slightly distorted from the geometries in the parent molecules, oxirane and benzene. Structural parameters for oxirane and benzene predicted by DFT/B3LYP/TZ2P calculations are given in Table 2. Differences between corresponding structural parameters are given in Table 1. In the case of the oxirane ring, the C−O bond lengths C2−O1 and C3−O1 of **1** are shortened by 0.001 Å and lengthened by 0.003 Å respectively from the (equal) values in oxirane. The C2−C3 bond length is increased by 0.009 Å. The ring angles change by <0.5°: the changes are 0.4°, −0.1°, and −0.3° for C2−O1−C3, O1−C2−C3, and O1−C3−C2, respectively. In the case of the phenyl ring, the largest changes in C−C bond length are for C7−C8 and C7−C12, which increase by 0.004 Å. C8−C9 and C11−C12 decrease by smaller amounts, 0.001 and 0.002 Å, respectively. C9−C10 and C10−C11 change very little: −0.001 and 0.000 Å, respectively. The ring angles C8−C7−C12 and C9−C10−C11 decrease by 0.9° and 0.4°, respectively. The other four angles increase by 0.1−0.6°. The ring is nonplanar: changes in CCCC dihedral angles range (in absolute value) from 0.0 to 0.9°. The largest changes are for C12−C7−C8−C9 and C11−C12−C7−C8 (0.9 and 0.7°, respectively). In both rings, C−H bond lengths[19] change very little: C3−H4 increases by 0.002 Å; all other changes are

(19) Ashvar, C. S. Ph. D. Thesis, University of Southern California, 1998, Chapter 6.

Table 2. Structural Parameters for Oxirane and Benzene[a]

	DFT						
	B3LYP/ TZ2P	B3PW91/ TZ2P[b]	B3LYP/ 6-31G*[b]	B3PW91/ 6-31G*[b]	MP2/ 6-31G*[b]	HF/SCF/ 6-31G*[b]	EXPT[c]
oxirane							
				Bond Length			
C−O	1.431	−8	−1	−8	8	−30	1.428 − 1.434
C−C	1.465	−3	4	0	0	−12	1.462 − 1.470
C−H	1.084	1	6	7	4	−7	1.085 − 1.086
				Bond Angles			
C−O−C	61.6	0.2	0.2	0.4	−0.4	0.8	61.62 − 61.67
O−C−C	59.2	−0.1	−0.1	−0.2	0.2	−0.4	
H−C−O	115.2	0	0.3	0.3	−0.1	0	
H−C−C	119.5	0	0.2	0.2	0.1	0.4	
H−C−H	115.7	0	−0.5	−0.4	−0.2	−0.5	116.28 − 116.92
benzene							
				Bond Lengths			
C−C	1.3913	−2.0	5.3	3.3	5.5	−5.1	1.3902 ± 0.0002
C−H	1.0817	1.4	5.3	5.6	5.7	−6.1	1.0862 ± 0.0015

[a] Bond lengths in Å, bond angles in degrees. [b] Differences (in 10^{-3} Å for bond lengths, degrees for angles) from DFT/B3LYP/TZ2P parameters. [c] From ref 20, for oxirane, ref 21 for benzene. For oxirane, the range is for the r_o, r_m, and r_s structures.

≤0.001 Å. Changes in HCC bond angles are <1° with the exception of H4−C3−C2 which decreases by 2.7°. H4−C3−O1 decreases by 1.5°, while H5−C2−O1 and H6−C2−O1 increase by 0.1°.

The change in energy of **1** with change in the dihedral angle, D, has been calculated. The results are shown in Figure 3. No further energy minima are found. The maximum energy corresponds to a tilted conformation, the direction of tilt taking H17 further from O1 than in the bisected conformation; D = 58°. The barrier height is 2.41 kcal/mol.

Vibrational unpolarized absorption and VCD spectra of **1** in CCl_4 and CS_2 solutions are shown in Figures 4−6. Vibrational frequencies, dipole strengths, and rotational strengths have been calculated for the predicted structure of **1**. The results are given in Table 3. Absorption and VCD spectra obtained thence are shown in Figures 6−8. Predicted and observed absorption spectra in the mid-IR (Figure 7) are in excellent qualitative agreement, allowing for the expected overall shift of the predicted spectrum to higher frequency, due in significant part to anharmonicity.[22] Assignment of the majority of fundamentals 7−37 follows straightforwardly, as indicated in Figure 7. Fundamentals 7, 8, 10, 13, 15, 16, 20−25, 28, 29, 32−35, and 37 are resolved and of sufficient intensity to permit unambiguous assignment. Fundamentals 9, 17, 26, 27, and 36 are very weak, as predicted, but definitely observable. Modes 11 and 12 are not resolved consistent with the predicted frequency separation of 7 cm^{-1}. Mode 14 is not observed, consistent with its predicted weak intensity and its proximity to the much stronger mode 13. Modes 18 and 19 are predicted to be split by 5 cm^{-1}; they are not resolved. The assignment of modes 30 and 31 is not straightforward: three bands are observed of comparable intensities; one is not a fundamental, or there is Fermi resonance. After assignment of the fundamentals of **1**, a number of bands remain unassigned; these are due either to nonfundamentals (overtone/combination) or to impurities.

Predicted and experimental VCD spectra in the mid-IR (Figure 8) are in good overall qualitative agreement, supporting the assignment arrived at from the absorption spectrum. The VCD of modes 20, 21, 23−25, 27−29, and 32−35 are clearly observed; except for mode 25, predicted and observed signs are in agreement. The observed VCD of mode 25 is weak and positive, although it is predicted to be weak and negative. Predicted and observed VCD of the unresolved modes 18 and 19 are also in agreement. The VCD intensities of modes 22, 26, 36, and 37 are predicted to be very weak; VCD is not clearly

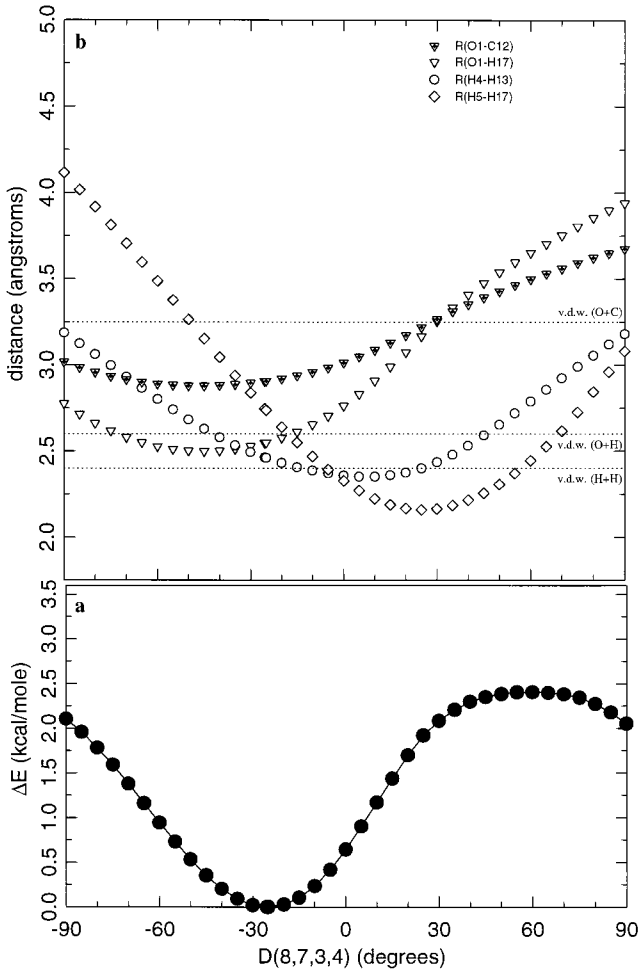

Figure 3. Variation in (a) energy and (b) interatomic distances as a function of the dihedral angle C8−C7−C3−H4, D, at the DFT/B3LYP/TZ2P level. van der Waals distances are obtained using van der Waals radii of C, 1.85 Å; O, 1.40 Å; H, 1.20 Å[29].

(20) Hirose, C. *Bull. Chem. Soc. Jpn.* **1974**, *47*, 1311.
(21) Pliva, J.; Johns, J. W. C.; Goodman, L. *J. Mol. Spectrosc.* **1991**, *148*, 427.
(22) Finley, J. W.; Stephens, P. J. *J. Mol. Struct. (THEOCHEM)* **1995**, *357*, 225.

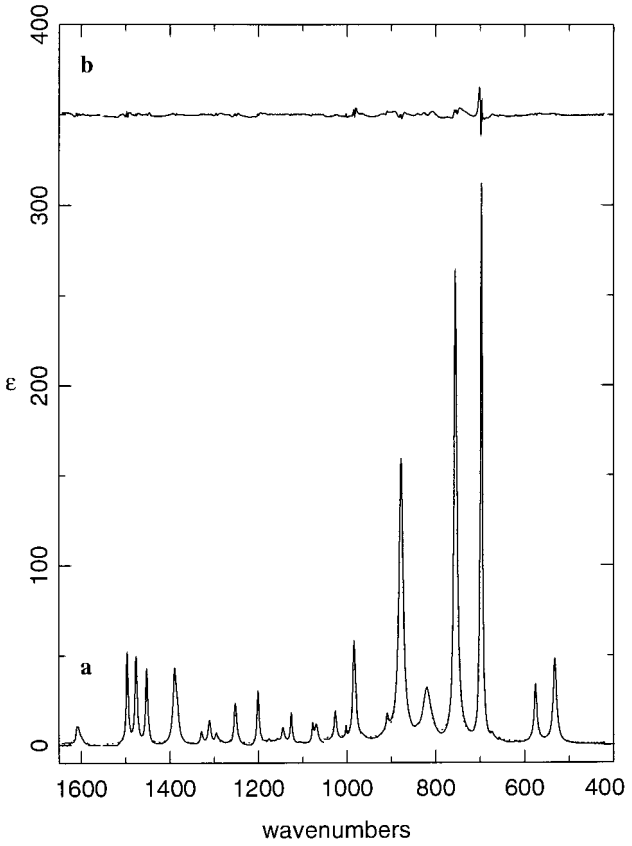

Figure 4. Mid-IR unpolarized absorption spectrum of **1**. (a) Solid line: experimental spectrum of S-(−)-**1** in CCl_4 (0.17 M, 1650−1050 cm^{-1}) and in CS_2 (0.16 M, 1050−400 cm^{-1}). Resolution is 1 cm^{-1}; path length is 505 micrometers. Dotted line: Lorentzian fit. (b) Experimental spectrum minus Lorentzian fit.

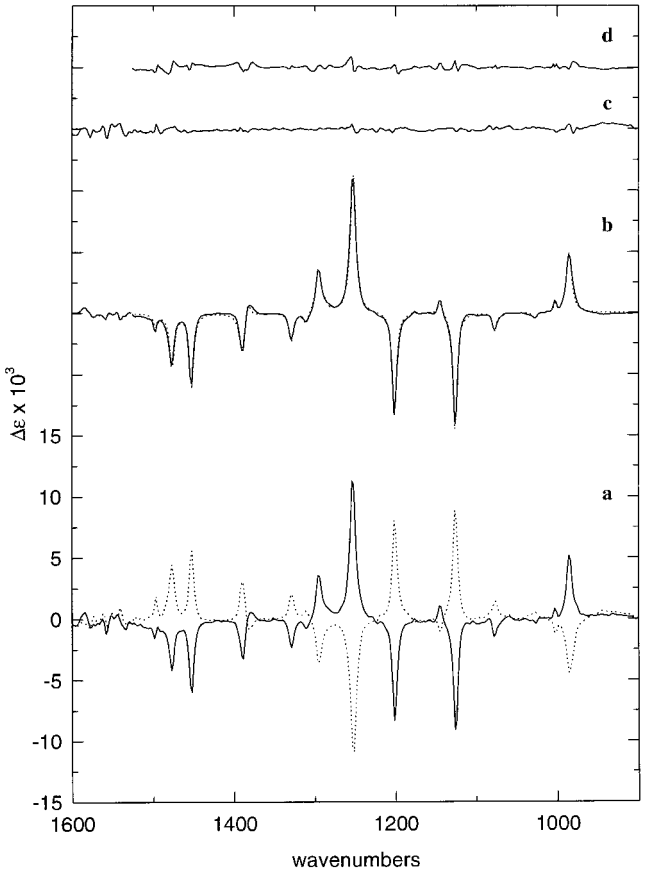

Figure 5. Mid-IR VCD spectrum of **1**. (a) Experimental spectra of S-(−)-**1** (solid line) and R-(+)-**1** (dotted line) in CCl_4 (0.71 M, 900−1600 cm^{-1}). Resolution is 4 cm^{-1}; path length is 300 μ. Scan times are 2 h. Baselines are the spectrum of (±)-**1** (0.71 M). (b) "Half-difference" spectrum (solid line), defined by $^1/_2[\Delta\epsilon(-) - \Delta\epsilon(+)]$, together with Lorentzian fit (dotted line) (900−1525 cm^{-1}). (c) "Half-sum" spectrum defined by $^1/_2[(\Delta\epsilon(-) + \Delta\epsilon(+)]$; this spectrum defines the experimental uncertainty in the half-difference spectrum. (d) Experimental half-difference spectrum minus Lorentzian fit.

detected for these modes. The triplet of bands near 1300 cm^{-1} gives bisignate VCD. Comparison to the calculated VCD strongly supports the assignment of the bands at 1295 and 1329 cm^{-1} to modes 30 and 31; the central band at 1311 cm^{-1} is then assigned as a nonfundamental.

Quantitative comparison of calculated and experimental frequencies, dipole strengths and rotational strengths for the bands assigned as fundamentals is shown in Figures 9−11. Experimental parameters are obtained via Lorentzian fitting; the fits are shown in Figures 4 and 5. The band corresponding to the overlapping unresolved modes 18/19 is fit with a single Lorentzian; for this band experimental dipole and rotational strengths are compared to combined calculated values. For all modes, calculated frequencies are greater than experimental frequencies. Percentage deviations range from 1.6 to 3.4%; the average percentage deviation is 2.4%. Predicted and experimental dipole strengths are in good agreement. The deviations are greatest for the bands originating in modes 10, 11, 12, and 15. For all of these bands, calculated dipole strengths are lower than experimental values. Predicted and experimental rotational strengths are also in good agreement.

DFT/B3LYP/TZ2P predicted frequencies and dipole strengths for oxirane and benzene are compared to gas-phase experimental values in Figures 12 and 13. The results for **1** in Figures 9 and 10 are comparable in accuracy.

DFT/B3PW91/TZ2P Calculations. The B3PW91 functional yields structural parameters very similar to those obtained using B3LYP (Table 1). The tilt angle is 14.6°, a difference of 0.1°. The dihedral angle, D, is 26.0°, a difference of 0.4°. The differences parallel those observed in oxirane and benzene (Table 2). B3PW91 oxirane and phenyl ring C−C bond lengths are shorter by 0.004 and 0.002 Å (cf. 0.003 Å in oxirane, 0.002 Å in benzene), C−O bond lengths are shorter by 0.008 Å (cf. 0.008 Å in oxirane), and C−H bond lengths[19] are longer by 0.001−0.002 Å (cf. 0.001 Å in oxirane and benzene) as compared to B3LYP values (Table 1). Differences between corresponding structural parameters in **1** and in oxirane and benzene are accordingly extremely similar for the two functionals (Table 1).

Predicted vibrational parameters (Table 3) and spectra (Figures 6−8) are also very similar to the B3LYP results. Qualitative differences in the predicted mid-IR absorption spectra are limited to modes 13 and 14; although their splitting is essentially identical (15−16 cm^{-1}), the relative intensities are reversed. Thus, the B3PW91 calculation would assign the band at 819 cm^{-1} to mode 14, mode 13 being unobserved. The lesser separation of modes 15 and 16 (15 cm^{-1} as opposed to 38 cm^{-1}) and the lower intensity of mode 31 are also noteworthy: in both cases, the B3LYP calculation is in superior agreement with experiment. For modes 18−37, qualitative differences in the predicted mid-IR VCD spectra occur for modes 30 and 31; the B3PW91 calculation is in much worse agreement with experiment. Qualitative differences also occur for modes 13 and 14; unfortunately, the VCD of these modes has not been observed.

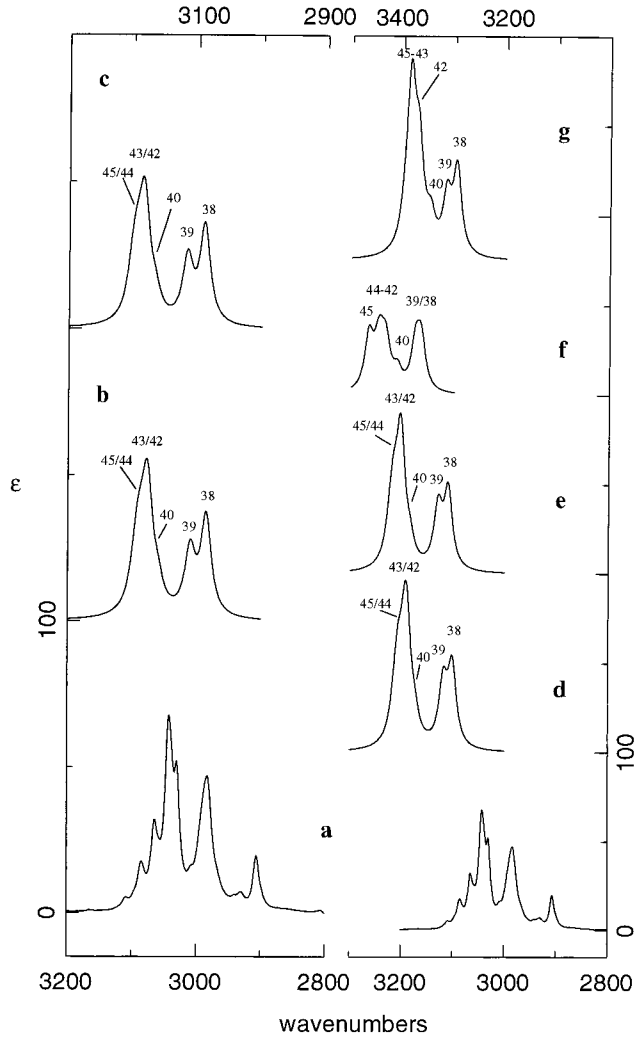

Figure 6. C−H stretching absorption spectrum of **1**. (a) Experimental spectrum in CS_2 (0.16 M). Resolution is 1 cm^{-1}; path length is 505 μ. (b−g) Calculated spectra; $\gamma = 10$ cm^{-1}. (b) DFT/B3LYP/TZ2P. (c) DFT/B3PW91/TZ2P. (d) DFT/B3LYP/6-31G*. (e) DFT/B3PW91/6-31G*. (f) MP2/6-31G*. (g) HF/SCF/6-31G*. The top scale of the left-hand panel applies to (b) and (c); the top scale of the right-hand panel applies to (g). Fundamentals are numbered.

With the exception of modes 13−15 and mode 30, B3PW91 frequencies for modes 1−35 are very close to B3LYP frequencies (<10 cm^{-1} difference). Modes 13, 14, 15, and 30 are predicted to be 14, 15, 21, and 11 cm^{-1} higher, respectively. When B3PW91 and experimental frequencies are compared (Figure 9), the percentage deviations for modes 14 and 15 are significantly larger than all other modes. We conclude that the B3PW91 calculation is less reliable for these modes than the B3LYP calculation. In particular, the assignment of the 819 cm^{-1} band to mode 13, mode 14 being too weak to be observed, arrived at from the B3LYP calculations, is clearly to be preferred to the assignment of the 819 cm^{-1} band to mode 14, mode 13 being too weak to be observed, resulting from the B3PW91 calculations. Overall, percentage deviations of calculated and experimental frequencies range from 1.8 to 7.0%; the average is 2.7%. B3PW91 and B3LYP calculated dipole and rotational strengths are in comparable agreement with experiment (Figures 10 and 11).

DFT/B3PW91/TZ2P frequencies and dipole strengths for oxirane and benzene are compared to experiment in Figures 12 and 13. Their accuracy is comparable to that of the B3LYP parameters with the notable exception of the 822 cm^{-1} mode of oxirane, for which B3PW91 gives a much larger percentage deviation in frequency. The relative accuracies of the B3PW91 and B3LYP results for **1** thus parallel the analogous results for oxirane and benzene.

DFT/B3LYP/6-31G* Calculations. B3LYP/6-31G* calculations yield structural parameters generally similar to the B3LYP/TZ2P results (Table 1). The tilt angle is 14.7°, a difference of 0.2°. The dihedral angle, D, is 26.3°, a difference of 0.7°. In oxirane and benzene (Table 2) 6-31G* C−C bond lengths are longer (0.004 Å in oxirane, 0.005 Å in benzene), and C−H bond lengths are longer (0.006 Å in oxirane, 0.005 Å in benzene). The C−O bond length of oxirane changes very little (−0.001 Å). The changes in **1** are very similar (Table 1). Differences between corresponding structural parameters in **1** and in oxirane and benzene are accordingly very similar for the two basis sets (Table 1).

Predicted vibrational parameters and spectra are given in Table 3 and Figures 6, 14 and 15. The mid-IR absorption spectrum is qualitatively very similar to the TZ2P spectrum. The largest differences are for modes 13/14 and 18/19. The splitting of modes 13 and 14 is reduced from 15 to 5 cm^{-1}, and the ratio of their intensities is greatly reduced. Conversely, the splitting of modes 18 and 19 is increased from 5 to 13 cm^{-1}, and the intensity ratio greatly shifted in favor of mode 19. In addition, the splitting of modes 34 and 35 is reduced from 11 to 2 cm^{-1}, and modes 7 and 10 suffer a substantial reduction in intensity. In comparison to the experimental spectrum, the 6-31G* spectrum is in poorer agreement. The relative intensities of the bands assigned to modes 7 and 8, and to 10 and 11/12 are better reproduced by the TZ2P calculation; the lack of resolution of mode 18 from 19 and the clear resolution of modes 34 and 35 are likewise more consistent with the TZ2P calculation. In the case of modes 13 and 14, the experimental absorption spectrum does not discriminate between the two calculations. The 6-31G* mid-IR VCD spectrum exhibits larger differences from the TZ2P spectrum: while the sign pattern is preserved, the intensity distribution for modes 13−16, 18/19, 24/25, 30/31, and 33−35 differs significantly; in addition, the VCD sign for mode 23 is reversed. In comparison to experiment, the agreement for the 6-31G* calculation is uniformly inferior.

Quantitatively, 6-31G* and TZ2P frequencies are very close (difference <10 cm^{-1}) for all modes <1250 cm^{-1}, with the exception of modes 13, 15, and 17 where the changes are 15, 16, and 22 cm^{-1}. The percentage deviations for modes 13 and 15 are significantly larger than those of other modes; for mode 17 the opposite is the case (Figure 9). We conclude that the 6-31G* calculation is less reliable for those modes than the TZ2P calculation. For modes above 1250 cm^{-1} the differences are greater, 6-31G* frequencies being uniformly higher. For all modes, percentage deviations of calculated frequencies from experiment lie in the range 0−6%. The average percentage deviation is 2.9%. The largest changes in predicted dipole and rotational strengths are for mode 10 and for modes 29 and 35, respectively; the 6-31G* values are in worse agreement with experiment.

DFT/B3LYP/6-31G* frequencies and dipole strengths for oxirane and benzene are compared to experiment in Figures 12 and 13. The basis set dependence of the results for **1** parallels that for the parent molecules.

DFT/B3PW91/6-31G* Calculations. The variation with basis set of B3PW91 structural parameters parallels that found with B3LYP (Table 1). The tilt angle is 15.1°, a difference of 0.5° from the TZ2P value. The dihedral angle, D, is 27.4°, a change of 1.4°. In oxirane and benzene, 6-31G* C−C bond

Table 3. Frequencies, Dipole Strengths and Rotational Strengths for Phenyloxirane[a]

experiment[b]				calculations															
				DFT/B3LYP/TZ2P			DFT/B3PW91/TZ2P			DFT/B3LYP/6-31G*			DFT/B3PW91/6-31G*			MP2/6-31G*		HF/SCF/6-31G*		
ν	D	R	fund.	ν	D	R	ν	D	R	ν	D	R	ν	D	R	ν	D	ν	D	R
			45	3196	10.0	1.9	3203	10.7	1.7	3213	10.7	0.9	3223	12.5	1.1	3266	26.1	3399	8.4	0.5
			44	3190	15.4	−0.7	3196	13.6	−0.9	3206	32.4	0.3	3216	27.0	−0.5	3250	9.8	3388	37.5	−0.1
			43	3180	16.8	−0.4	3187	14.0	−0.2	3194	34.1	0.5	3205	29.0	0.9	3244	17.2	3385	41.7	−6.4
			42	3176	23.4	−3.5	3184	22.4	−3.4	3188	41.4	−8.8	3201	38.2	−8.5	3233	20.9	3371	43.0	0.2
			41	3170	0.3	−0.1	3177	0.3	−0.2	3183	0.7	0.1	3195	0.6	0.0	3224	0.3	3359	2.4	−0.1
			40	3160	7.1	−0.7	3167	6.5	−0.5	3173	11.0	−0.5	3184	10.1	−0.4	3211	9.0	3348	13.8	0.1
			39	3110	20.1	−3.9	3117	19.9	−4.3	3118	31.7	−8.3	3129	30.7	−8.5	3176	22.9	3316	26.2	−11.9
			38	3086	31.5	−0.5	3090	30.8	0.8	3100	41.2	2.3	3110	40.0	3.2	3165	24.6	3297	41.4	−0.1
1608	7.5		37	1647	10.5	−0.5	1659	11.0	−0.5	1667	7.4	−0.1	1678	8.0	−0.2	1683	4.8	1815	6.7	−0.3
1601	1.3																			
1586	0.1		36	1626	0.8	0.4	1638	0.7	0.4	1645	0.4	0.2	1657	0.4	0.2	1662	0.4	1787	1.0	0.3
1496	23.1	−1.6	35	1535	25.7	−0.3	1535	24.1	−0.7	1549	14.7	−11.0	1551	16.5	−8.9	1572	9.5	1688	17.2	−15.8
1477	26.9	−7.5	34	1524	15.5	−10.7	1521	22.7	−12.2	1547	19.5	−2.1	1547	22.2	−5.0	1558	21.5	1673	27.3	−0.6
1452	22.2	−9.7	33	1491	19.2	−3.5	1489	17.6	−3.3	1503	23.4	−0.8	1503	23.6	−0.8	1513	30.3	1622	34.5	−1.1
1389	35.0	−8.6	32	1419	32.6	−5.9	1421	36.6	−4.2	1436	42.3	−6.1	1441	43.4	−4.9	1478	6.0	1565	62.4	−4.7
1383	9.7	3.8																		
1329	3.6	−4.2	31	1358	7.4	−4.0	1361	0.4	2.1	1366	2.2	−0.1	1381	1.0	4.0	1448	33.2	1471	11.2	−2.3
1311	9.7	−2.2																		
1295	4.9	8.3	30	1329	10.2	8.3	1340	14.1	0.9	1346	13.8	6.6	1349	12.7	1.4	1363	12.5	1412	23.1	20.5
1288	0.7	0.8																		
1252	18.3	26.0	29	1279	19.2	18.2	1284	21.0	22.6	1294	16.1	13.3	1300	18.5	16.7	1311	11.2	1348	7.9	−5.7
1201	19.6	−16.2	28	1220	12.0	−8.9	1226	10.7	−9.2	1229	10.2	−5.5	1236	10.1	−6.6	1253	11.6	1321	4.8	−5.4
1177	2.0	0.4	27	1203	0.9	0.7	1198	1.1	0.8	1209	1.9	1.1	1208	2.0	1.2	1229	3.2	1303	7.2	5.6
1157	1.8	−0.1	26	1186	0.3	0.1	1182	0.3	0.1	1193	0.4	0.1	1192	0.4	0.1	1216	0.6	1297	2.2	2.5
1144	8.1	2.6	25	1171	4.2	−0.7	1168	4.4	0.0	1178	4.1	−1.5	1178	4.4	−1.6	1194	4.1	1288	6.0	0.1
1126	11.1	−19.4	24	1151	6.7	−7.0	1149	7.7	−8.9	1152	3.3	−1.9	1153	4.2	−3.7	1169	4.9	1223	4.0	2.6
1106	0.6																			
1077	6.3	−2.8	23	1105	9.4	−1.0	1105	11.7	−1.2	1110	8.3	0.4	1112	11.5	−0.1	1125	7.7	1209	6.1	−0.2
1069	12.1	−0.4	22	1092	8.8	−0.1	1093	9.1	−0.4	1096	7.6	−1.2	1097	7.7	−1.6	1112	7.0	1181	9.2	−2.1
1026	12.5	−1.2	21	1051	12.4	−0.2	1054	14.6	−0.3	1057	8.2	−0.3	1061	10.8	−0.5	1068	9.0	1131	1.2	−0.5
1002	2.6	0.7	20	1022	2.7	1.0	1020	0.6	0.3	1018	0.7	0.1	1018	6.9	1.6	1026	27.4	1128	4.5	−0.7
			19	1011	12.2	1.9	1011	36.5	6.9	1011	47.3	11.6	1014	50.3	13.1	1024	18.2	1115	65.3	6.5
983	56.5	14.4																		
			18	1006	42.6	9.4	1007	28.5	6.9	998	3.8	1.3	999	3.4	1.3	923	137.5	1104	0.8	0.3
966	0.2		17	994	0.0	0.0	993	0.0	0.0	972	0.2	−0.2	975	0.2	−0.1	901	2.4	1089	0.7	−0.5
909	9.9		16	934	6.2	−1.2	932	5.3	−1.3	928	3.5	−4.6	932	95.2	1.1	892	3.3	1038	20.0	1.6
877	275.5		15	896	154.3	6.6	917	142.0	7.0	912	135.5	13.0	927	37.0	5.1	876	70.5	1003	125.4	10.9
			14	862	1.2	4.5	877	94.3	−1.2	867	33.9	4.1	893	102.6	0.9	870	6.0	987	130.4	−0.7
819[c]	96.1[c]		13	847	89.2	−14.2	861	3.0	−5.3	862	63.3	−7.0	864	1.6	−1.6	838	1.5	961	0.8	−1.7
755	270.5		12	772	197.7	13.2	773	199.8	12.3	773	174.6	9.4	772	170.5	2.4	778	18.8	852	227.9	11.8
752	96.3		11	765	42.0	20.3	768	22.8	14.5	767	30.1	11.6	770	48.4	16.9	739	368.3	822	32.3	19.8
696	295.3		10	715	223.8	−1.9	714	230.1	−1.0	714	111.8	−1.7	713	140.4	−0.7	632	0.1	778	133.4	−3.5
673	2.3																			
664	0.4																			
655	0.7																			
619	0.1		9	636	0.1	−0.2	630	0.1	−0.2	634	0.1	−0.2	630	0.1	−0.3	591	57.2	678	0.1	−0.3
575	57.3		8	588	54.4	15.4	586	50.5	14.2	587	55.6	12.3	586	53.3	12.9	570	51.0	630	68.4	20.2
531	109.3		7	545	87.9	−0.5	544	92.0	0.2	545	49.4	−0.8	544	61.4	−1.2	491	29.3	593	70.0	−5.4
			6	416	1.5	0.0	413	1.6	0.0	418	1.7	0.0	415	1.8	0.1	403	15.0	456	0.9	0.2
			5	397	14.9	4.4	398	13.3	4.6	399	12.4	3.4	401	11.5	3.8	397	0.2	435	17.5	4.4
			4	337	12.5	6.5	335	11.5	6.2	339	10.6	7.4	336	9.9	6.8	331	13.2	363	9.4	6.8
			3	196	84.5	−7.2	192	86.5	−9.0	197	88.8	−7.1	194	92.3	−9.2	205	102.3	217	108.1	−12.0
			2	147	66.3	3.5	145	60.7	3.6	148	48.4	4.0	147	49.8	3.8	144	54.5	158	46.5	4.0
			1	58	191.5	−25.5	60	174.1	−24.1	67	159.1	−24.2	68	155.8	−23.1	67	168.3	62	254.4	−21.8

[a] Frequencies in cm^{-1}; dipole strengths in 10^{-40} esu^2 cm^2; rotational strengths in 10^{-44} esu^2 cm^2. [b] Frequencies and dipole strengths from 1 cm^{-1} resolution CCl_4 spectra >1050 cm^{-1} and CS_2 spectra <1050 cm^{-1}. Rotational strengths from 4 cm^{-1} resolution CCl_4 spectra. Bands not assigned to fundamentals of **1** are attributable either to nonfundamentals of **1** or to impurities. [c] The band at 819 cm^{-1} is assigned to fundamental 13; fundamental 14 is not observed: see text.

lengths are 0.003 and 0.005 Å longer, and C−H bond lengths are 0.006 and 0.004 Å longer, respectively (Table 2). In oxirane, the C−O bond length is unchanged. The changes in **1** are very similar. The differences between corresponding parameters in **1** and oxirane and benzene are very similar to the B3LYP/6-31G* values (Table 1).

Predicted vibrational parameters and spectra are given in Table 3 and Figures 6, 14 and 15. The mid-IR absorption spectrum is qualitatively very similar to the TZ2P spectrum. The largest differences are for modes 15/16 and 18−20. The splitting of modes 15 and 16 is reduced to 5 cm^{-1} from 15 cm^{-1} and the intensities become much more similar. The splitting of modes 18 and 19 is increased to 15 cm^{-1} from 4 cm^{-1} and the relative intensity of mode 18 substantially decreased. At the same time, the splitting of modes 19 and 20 decreases from 9 to 4 cm^{-1}. In addition, the intensities of modes 7, 10, and 15 are significantly decreased. The 6-31G* calculations are uniformly in worse agreement with experiment. The largest qualitative changes in the mid-IR VCD spectra of modes 18−37 are for modes 18−20 and 23−25. The intensities of modes 18, 19, and 20 decrease, increase, and increase, respectively. The intensities of modes 23, 24, and 25 decrease,

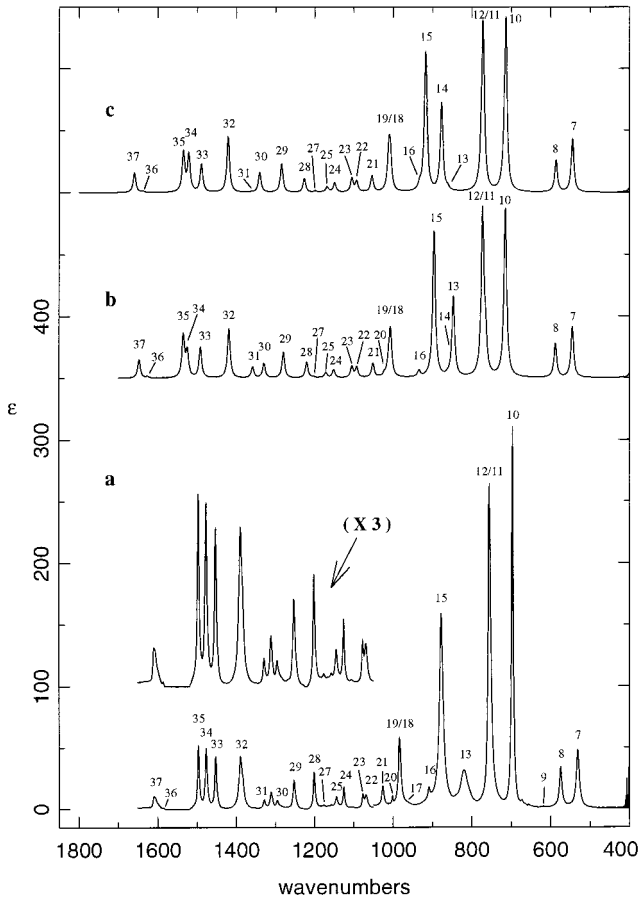

Figure 7. Mid-IR absorption spectrum of **1**. (a) Experimental spectrum (from Figure 4). (b−c) Calculated spectra are (b) DFT/B3LYP/TZ2P; (c) DFT/B3PW91/TZ2P; $\gamma = 4$ cm^{-1}. Fundamentals are numbered.

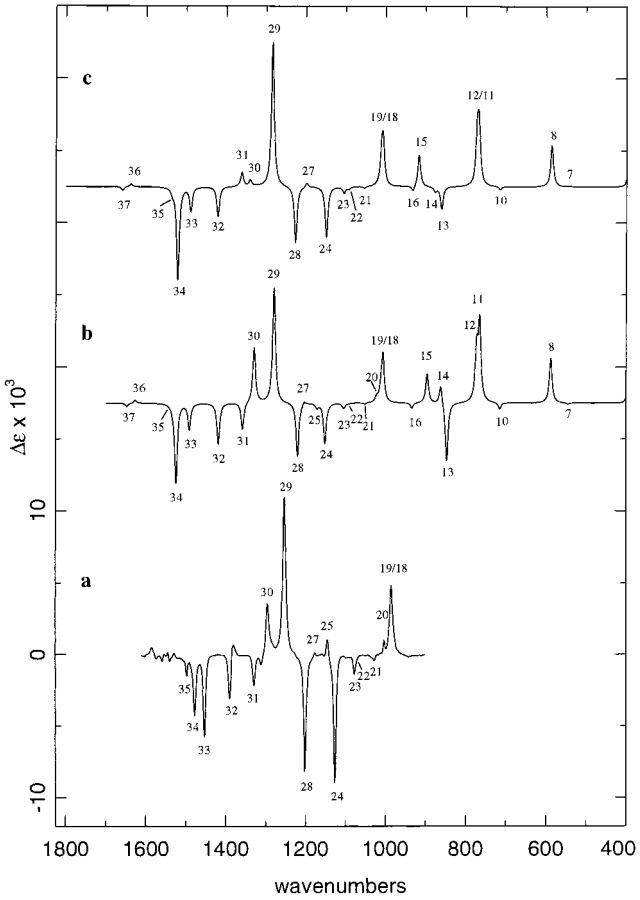

Figure 8. Mid-IR VCD spectrum of S-(−)-**1**. (a) Experimental spectrum (half-difference spectrum of Figure 5). (b−c) Calculated spectra are (b) DFT/B3LYP/TZ2P; (c) DFT/B3PW91/TZ2P; $\gamma = 4$ cm^{-1}. Fundamentals are numbered.

decrease, and increase, respectively. The 6-31G* calculation is in worse agreement with experiment for all of these modes.

Quantitatively, 6-31G* and TZ2P frequencies are very close (difference ≤ 10 cm^{-1}) for all modes <1250 cm^{-1} with the exception of modes 14 and 17, which differ by 16 and 18 cm^{-1}, respectively. For modes above 1205 cm^{-1} the differences are greater, 6-31G* frequencies being uniformly higher. Percentage deviations lie in the range 0−6%; the average is 3.1%. Agreement of calculated dipole and rotational strengths is worse than at the TZ2P level.

DFT/B3PW91/6-31G* frequencies and dipole strengths for oxirane and benzene are compared to experiment in Figures 12 and 13. The basis set dependence of the results for **1** parallels that for the parent molecules.

MP2/6-31G* Calculations. MP2/6-31G* structural parameters are given in Table 1. The tilt angle is 14.9°. The differences from corresponding parameters in oxirane and benzene (Table 2) are very similar to those predicted using DFT (Table 1). The largest differences between DFT and MP2 results are in the oxirane C−O bond lengths C2−O1 and C3−O1 which are 0.009 and 0.011 Å longer than the DFT/B3LYP/TZ2P values and 0.017 and 0.019 Å longer than the DFT/B3PW91/TZ2P values.

Predicted vibrational parameters and spectra are given in Table 3 and Figures 6 and 14. The predicted mid-IR absorption spectrum is overall qualitatively very different from the DFT spectra (Figures 7 and 14). For modes 21−30 and 33−37 the difference is not large. However, for modes 7−20 and 31−32, the differences are very large. The MP2 calculation is in much worse agreement with experiment. From the MP2 calculation alone, the experimental spectrum below 1000 cm^{-1} could not be assigned.

Quantitative comparison of the MP2 frequencies and dipole strengths to experimental values (Figures 9 and 10) further exposes the drastically lower accuracy of the MP2 results. The percentage errors in predicted frequencies for modes at <1000 cm^{-1} vary wildly in the range +5 to −10%. Above 1000 cm^{-1} the errors are more similar to those for the DFT/6-31G* calculations, except for mode 31. The average (absolute) percentage deviation is 4.5%. Calculated and experimental dipole strengths exhibit almost no correlation.

Rotational strengths and VCD intensities have not been calculated since MP2 AATs are not available. The errors in the MP2 HFF would lead to major errors in MP2 rotational strengths and VCD intensities for those modes whose dipole strengths and absorption intensities are in error. The MP2 VCD spectrum would therefore be in poor agreement with experiment.

MP2/6-31G* frequencies and dipole strengths for oxirane and benzene are compared to experiment in Figures 12 and 13. The agreement of calculated and experimental frequencies for oxirane is comparable to that of the DFT/6-31G* calculations. In contrast, MP2/6-31G* frequencies for benzene vary dramatically in accuracy and, overall, are in much worse agreement with experiment than DFT/6-31G* frequencies. For one mode (707 cm^{-1}) the percentage deviation is nearly −30%. The deficiencies of MP2 in predicting vibrational frequencies in multiply bonded molecules, including benzene, are well-known[26] and need no further discussion. The agreement of calculated

(23) Nakanaga, T. *J. Chem. Phys.* **1980**, *73*, 5451; **1981**, *74*, 5384.

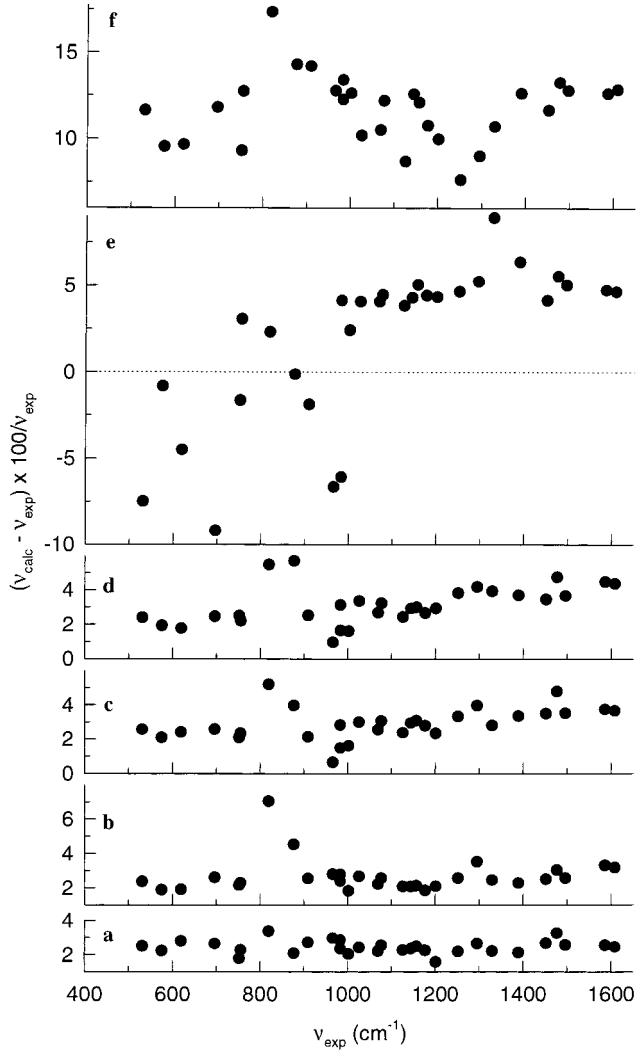

Figure 9. Comparison of calculated and experimental frequencies of **1**. (a) DFT/B3LYP/TZ2P; (b) DFT/B3PW91/TZ2P; (c) DFT/B3LYP/6-31G*; (d) DFT/B3PW91/6-31G*; (e) MP2/6-31G*; (f) HF/SCF/6-31G*. Modes 13 are compared to the 819 cm^{-1} experimental band except in (b) where mode 14 is compared.

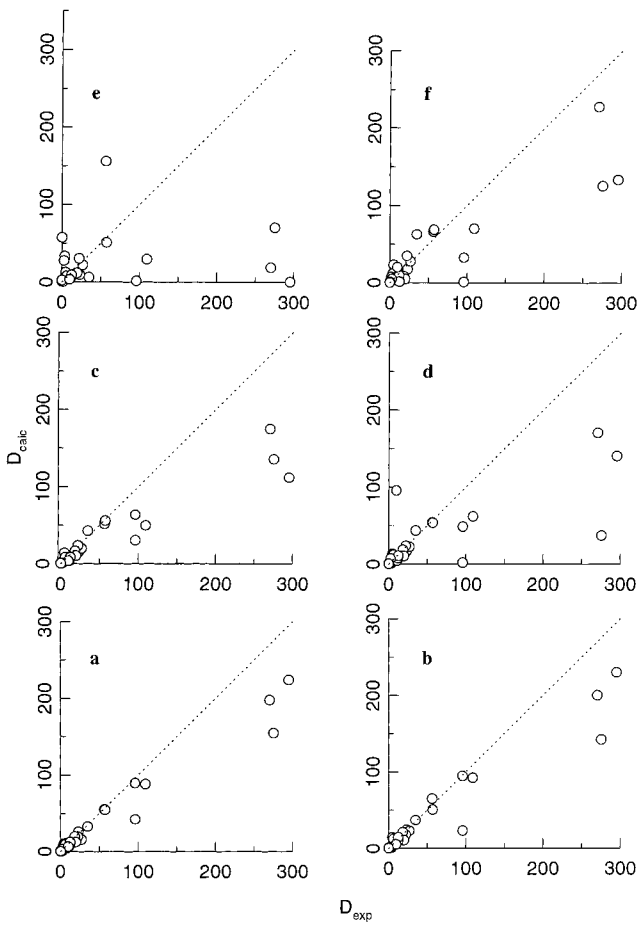

Figure 10. Comparison of calculated and experimental dipole strengths of **1**. (a) DFT/B3LYP/TZ2P; (b) DFT/B3PW91/TZ2P; (c) DFT/B3LYP/6-31G*; (d) DFT/B3PW91/6-31G*; (e) MP2/6-31G*; (f) HF/SCF/6-31G*. Dipole strengths are in 10^{-40} esu^2 cm^2. The diagonal line has a slope of +1. Modes 13 are compared to the 819 cm^{-1} experimental band except in (b) where mode 14 is compared.

and experimental dipole strengths for both oxirane and benzene is comparable to that of the DFT/6-31G* calculations. For benzene, only a_{2u} and e_{1u} modes are IR-allowed; for these modes predicted frequencies are of "normal" accuracy.

The much lower accuracy of MP2 for **1**, relative to DFT, reflects the inadequacy of MP2 in predicting the harmonic force field of benzene.

HF/SCF/6-31G* Calculations. HF/SCF/6-31G* structural parameters are given in Table 1. The tilt angle is 18.0°. The differences from corresponding parameters in oxirane and benzene (Table 2) are very similar to those predicted using DFT and MP2 (Table 1). All HF/SCF bond lengths are shorter than DFT bond lengths. The largest differences are in the oxirane C−O bond lengths C2−O1 and C3−O1, which are 0.027 and 0.032 Å shorter than the DFT/B3LYP/TZ2P values and 0.019 and 0.024 Å shorter than the DFT/B3PW91/TZ2P values.

Predicted vibrational parameters and spectra are given in Table 3 and Figures 6, 14 and 15. The predicted mid-IR absorption spectrum (Figure 14) is shifted overall to higher frequencies than the DFT spectra. The pattern of frequencies and intensities differs substantially from the DFT results and is in worse agreement with experiment. Quantitative comparison of calculated and experimental frequencies (Figure 9) shows a wide variation in percentage errors within the range 7−18%; the average percentage deviation is 11.7%. Calculated and experimental dipole strengths are in poor agreement (Figure 10).

The predicted mid-IR VCD spectrum (Figure 15) differs even more from the DFT spectra and is in even worse agreement with experiment. As shown in Figure 11, calculated and experimental rotational strengths show very little correlation.

HF/SCF/6-31G* frequencies and dipole strengths for oxirane and benzene are compared to experiment in Figures 12 and 13. The accuracy of the HF/SCF/6-31G* frequencies for **1** is comparable to that for the parent molecules.

C−H Stretching Spectrum. The experimental C−H stretching absorption spectrum is shown in Figure 6, together with the DFT, MP2, and HF/SCF spectra. Modes 38 and 39 are the oxirane CH_2 symmetric stretch and the CH stretch throughout. The oxirane CH_2 asymmetric stretch is mode 42 in the DFT

(24) Goodman, L.; Ozkabak, A. G.; Thakur, S. N. *J. Phys. Chem.* **1991**, *95*, 9044; see also: Ashvar, C. S. Ph. D. Thesis, University of Southern California, 1998, Chapter 5.

(25) Goodman, L.; Ozkabak, A. G.; Wiberg, K. B. *J. Chem. Phys.* **1989**, *91*, 2069; Akiyama, M.; Shimizu, Y.; Itaya, H.; Kakihana, M. *J. Phys. Chem.* **1989**, *93*, 2280; see also: Ashvar, C. S. Ph. D. Thesis, University of Southern California, 1998, Chapter 5.

(26) Simandiras, E. D.; Rice, J. E.; Lee, T. J.; Amos, R. D.; Handy, N. C. *J. Phys. Chem.* **1988**, *88*, 3187. Handy, N. C.; Maslen, P. E.; Amos, R. D.; Andrews, J. S.; Murray, C. W.; Laming, G. J. *Chem. Phys. Lett.* **1992**, *197*, 506. Handy, N. C.; Murray, C. W.; Amos, R. D. *J. Phys. Chem.* **1993**, *97*, 4392.

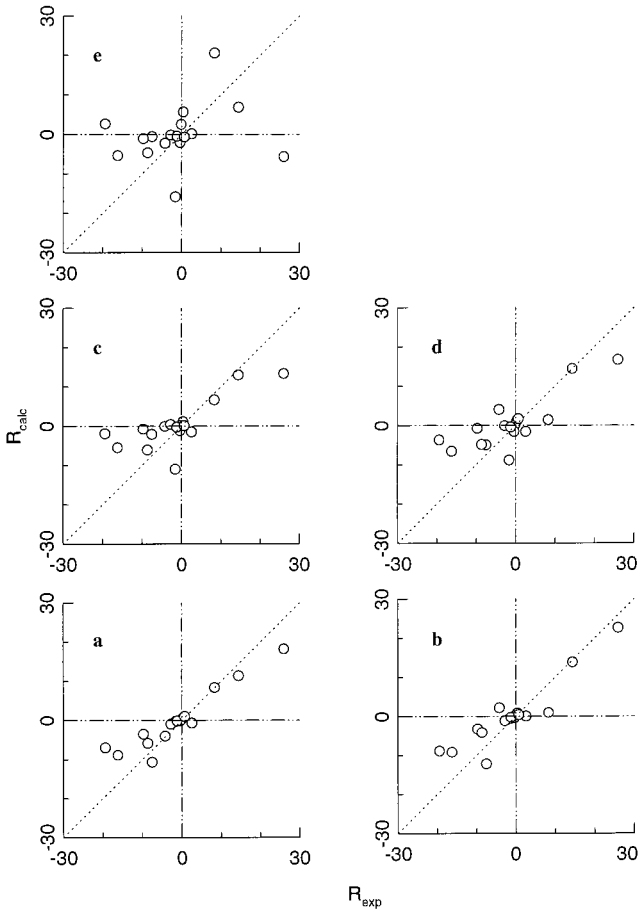

Figure 11. Comparison of calculated and experimental rotational strengths of **1**. (a) DFT/B3LYP/TZ2P; (b) DFT/B3PW91/TZ2P; (c) DFT/B3LYP/6-31G*; (d) DFT/B3PW91/6-31G*; (e) HF/SCF/6-31G*. Rotational strengths are in 10^{-44} esu^2 cm^2. The diagonal line has a slope of +1.

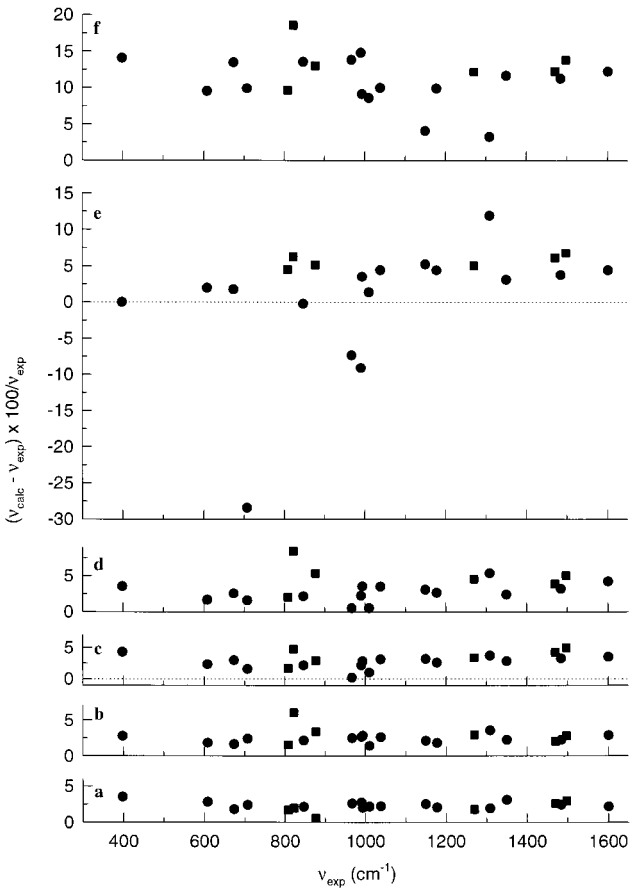

Figure 12. Comparison of calculated and experimental frequencies of oxirane (■) and benzene (●). (a) DFT/B3LYP/TZ2P; (b) DFT/B3PW91/TZ2P; (c) DFT/B3LYP/6-31G*; (d) DFT/B3PW91/6-31G*; (e) MP2/6-31G*; (f) HF/SCF/6-31G*. Experimental frequencies for oxirane and benzene are from refs 23 and 24, respectively.

calculations, mode 44 and mode 45 in the MP2 and HF/SCF calculations. The remaining modes are phenyl C−H stretches. The assignment of the gas-phase spectrum of oxirane[23] leads to assignment of observed bands of **1** at <3000 cm^{-1} to oxirane symmetric CH_2 and CH modes, in Fermi resonance with nonfundamentals at lower frequency. The bands at >3000 cm^{-1} are assigned to the phenyl C−H stretching modes together with the oxirane CH_2 asymmetric stretch. In view of the complexity of the experimental spectrum and the importance of anharmonicity we have not attempted a more detailed assignment.

Discussion

A number of criteria can be used to assess the accuracy of predictions of unpolarized absorption and VCD spectra: the qualitative agreement of predicted and experimental spectra; the quantitative agreement of predicted and experimental frequencies, dipole strengths, and rotational strengths. By all of these measures the DFT/B3LYP/TZ2P calculation is the most accurate of the six calculations carried out. There are no major qualitative differences between predicted and observed mid-IR spectra. Calculated vibrational frequencies of modes 7−37 (excepting 14 which is not observed) differ from observed frequencies by 1.6−3.4%, on average 2.4%. Dipole and rotational strengths are in excellent qualitative agreement. The DFT/B3PW91/TZ2P calculation provides results of lower accuracy, but the difference is not large. In particular, the average percentage deviation of frequencies is increased but only to 2.7%. 6-31G* calculations are less accurate than TZ2P calculations. The average percentage deviations of frequencies for B3LYP and B3PW91 are 2.9 and 3.1%, respectively. MP2/6-31G* and HF/SCF/6-31G* calculations are of substantially lower accuracy; average percentage deviations of frequencies are 4.5 and 11.7%, respectively. The accuracy of predicted dipole and rotational strengths qualitatively tracks the accuracy of the calculated frequencies.

The relative accuracies of the predicted equilibrium geometries parallel those of the predicted vibrational spectra. It follows that the DFT/B3LYP/TZ2P geometry is the most accurate. Its absolute accuracy is less easily defined, since there is no direct method for converting frequency deviations into errors in bond lengths and angles. Comparison of the TZ2P calculations using B3LYP and B3PW91 provides some insight into likely error bounds. First, we note that all differences in bond length are <0.01 Å and that two are much larger than all others: the oxirane ring C−O bond lengths differ by 0.008 Å (being shorter for B3PW91). Second, we note that substantial differences in frequencies, dipole strengths, and rotational strengths are localized to modes 13−15 and 30−31, B3PW91 frequencies, dipole strengths and rotational strengths all being clearly less accurate than B3LYP values. Examination of these modes is consistent with strong participation of the oxirane ring deformation coordinates. (Note that the ring deformation modes of oxirane occur at 822, 877, and 1270 cm^{-1}.[23]) Thus, a change of 0.008 Å in C−O bond length effects an observable deterioration in the accuracy of vibrational frequencies, normal coordinates and intensities, while the changes in C−C and C−H bond lengths (≤0.004 Å) do not. A reasonable conclusion is that the

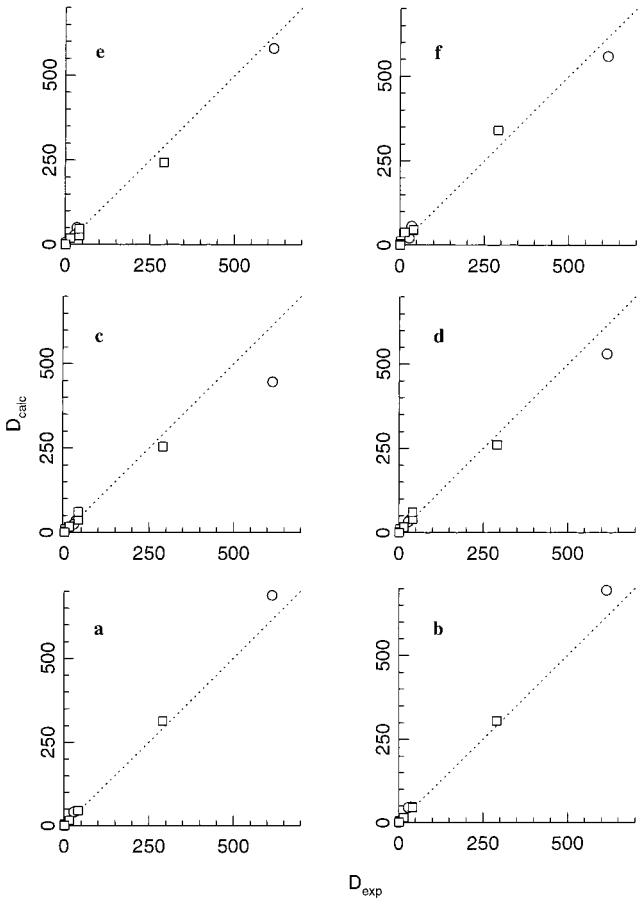

Figure 13. Comparison of calculated and experimental dipole strengths of oxirane (□) and benzene (○). (a) DFT/B3LYP/TZ2P; (b) DFT/B3PW91/TZ2P; (c) DFT/B3LYP/6-31G*; (d) DFT/B3PW91/6-31G*; (e) MP2/6-31G*; (f) HF/SCF/6-31G*. Experimental intensities for oxirane and benzene are from refs 23 and 25, respectively.

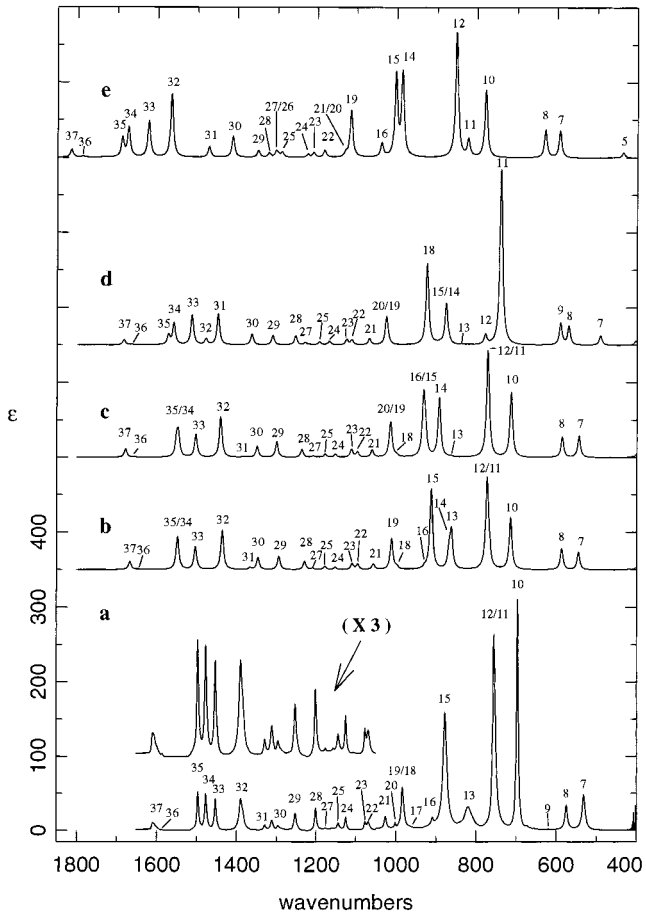

Figure 14. Mid-IR absorption spectrum of **1**. (a) Experimental spectrum (from Figure 4). (b−e) Calculated spectra are (b) DFT/B3LYP/6-31G*; (c) DFT/B3PW91/6-31G*; (d) MP2/6-31G*; (e) HF/SCF/6-31G*; $\gamma = 4$ cm^{-1}. Fundamentals are numbered.

accuracy of the bond lengths is in the range 0.004−0.008 Å. With regard to bond angles, we note that all differences in bond angle are ≤ 0.3°, with no angle differing much more than all others. Likewise, differences in torsional angles lie in the range 0−1°, the largest being 0.8°. We conclude that lower limits to the accuracies of bond angles and torsional angles are 0.3° and 1°, respectively. However, we cannot infer upper limits in this way.

These estimates can be refined by consideration of the differences between DFT/TZ2P structural parameters for **1** and for oxirane and benzene together with the differences between calculated and experimental parameters for the latter molecules (Table 2). We have shown that the differences between structural parameters calculated for **1** and for oxirane and benzene are essentially identical at all calculational levels. This implies that the errors in calculated parameters in **1** must be identical to those of the corresponding parameters of benzene and oxirane. Experimental structures exist for oxirane[20] and benzene,[21] and the accuracy of DFT/TZ2P structural parameters can be assessed directly. For the C−O and C−C bond lengths of oxirane, B3LYP values lie within the ranges 1.428−1.434 Å and 1.462−1.470 Å of the r_o, r_m, and r_s values,[20] as also does the B3PW91 C−C bond length. However, the B3PW91 C−O value, 1.423 Å, is significantly outside the experimental range (on the low side). For the C−H bond lengths the experimental range is 1.085−1.086, compared to B3LYP and B3PW91 values of 1.084 and 1.085 Å. B3LYP and B3PW91 C−C bond lengths in benzene err by 0.0011 and −0.0009 Å respectively, while C−H bond lengths err by −0.0045 and −0.0031 Å. The quoted experimental errors are 0.0002 and 0.0015 Å, respectively.[21] This comparison shows that the errors in all calculated bond lengths are <0.005 Å with the exception of the B3PW91 C−O bond length for which the error may be as great as −0.011 Å. With regard to the HCH angle of oxirane, the experimental range is 116.3−116.9° compared to the B3LYP and B3PW91 values of 115.7°, a difference of 0.6−1.2°. The comparison of calculated and experimental structural parameters for benzene and oxirane supports the conclusions that for **1** (1) the primary difference in accuracy of the TZ2P B3LYP and B3PW91 structures lies in the C−O bond lengths, the B3PW91 prediction being significantly less accurate; (2) errors in other bond lengths are probably <0.005 Å; (3) errors in bond angles are probably <2°. These conclusions are consistent with those arrived at above.

We turn now to the changes in the two rings of **1** from their geometries in the two parent molecules. As demonstrated above, all calculations predict the same changes, qualitatively and quantitatively. It is very likely, therefore, that more accurate calculations will (to an accuracy of ∼0.001 Å and 0.1° at least) also yield identical results. Both rings lose their parental symmetry. Not surprisingly, the changes are greatest close to atoms C3 and C7. Thus, C3−O1 is changed more than C2−O1, C7−C8 more than C8−C9 and C9−C10, C2−C3−H4 more than C3−C2−H6, C12−C7−C8 more than C8−C9−C10, and so on. The bond lengths C7−C8, C7−C12, C2−C3, and C3−O1 are all lengthened, indicating a lowering of bond order. These

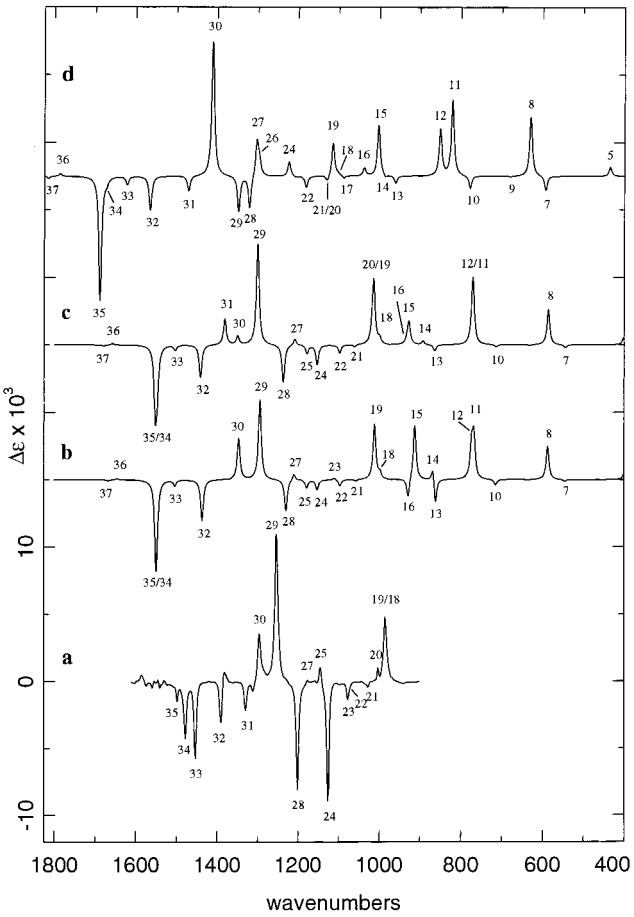

Figure 15. Mid-IR VCD spectrum of S-(−)-**1**. (a) Experimental spectrum (half-difference spectrum of Figure 5). (b−d) Calculated spectra are (b) DFT/B3LYP/6-31G*; (c) DFT/B3PW91/6-31G*; (d) HF/SCF/6-31G*; $\gamma = 4$ cm^{-1}. Fundamentals are numbered.

changes are consistent with the presence of pseudoconjugation between the rings, as further discussed below.

The tilt angle, the difference from 90° of the angle between the O1−C2−C3 and C7−C8−C12 planes, is 14.5−15.1° for the DFT calculations, 14.9° for the MP2/6-31G*, and 18.0° for HF/SCF/6-31G*. The dihedral angle D is 25−26° for the DFT/TZ2P calculations, 26−28° for DFT/6-31G*, and 30.5 and 33.0° at the MP2/6-31G* and HF/SCF/6-31G* levels, respectively. The most accurate calculation gives the smallest values of the tilt angle and of D. The bond length of the inter-ring C3−C7 bond lies in the range 1.485−1.495 Å for all calculations, greater than the C−C bond lengths for the two rings as expected.

There has been much discussion of conjugation between the phenyl and cyclopropane rings of phenylcyclopropane.[8,27] This pseudoconjugation favors the bisected conformation, in which the tilt angle and the dihedral angle D are 0°, over the perpendicular conformation, in which the dihedral angle D is 90°. The former is observed experimentally by X-ray crystallography.[28] Pseudoconjugation would be expected to operate likewise in **1** leading to a preference for a conformation with tilt and dihedral angles near 0° (recognizing the reduced symmetry of **1** relative to phenylcyclopropane). Indeed, values close to 0° are predicted. Is this due to pseudoconjugation? We answer this question by comparing the structures of **1** obtained by optimization at D values of 0° and 90° to that of the equilibrium structure. DFT/B3LYP/TZ2P bond lengths are compared in Table 4. The important bond length is C3−C7. At D = 0° and D = 90°, values are 1.487 and 1.495 Å, respectively. At the optimized geometry, it is 1.488 Å. Thus, it is shortest at D = 0°, a little longer (0.001 Å) at D = 25.6°, and substantially longer (0.008 Å) at D = 90°. The shortening of C3−C7 as D varies from 90 to 0° is reasonably attributed to increasing conjugation between the two rings. The value of C3−C7 in the optimized geometry is much closer to that at D = 0° than to that at D = 90°, leading to the conclusion that such conjugation is not substantially diminished as D increases to 25.6°.

Table 4. Effects of Internal Rotation on the Structural Parameters for Phenyloxirane[a]

	D		
bond lengths	25.6°	0°	90°
1,2	1.430	1.429 (−1)[b]	1.433 (3)[b]
1,3	1.433	1.438 (5)	1.435 (2)
2,3	1.474	1.472(−2)	1.467 (−7)
3,7	1.488	1.487 (−1)	1.495 (7)
7,8	1.395	1.394 (−1)	1.394 (−1)
8,9	1.390	1.391 (1)	1.390 (0)
9,10	1.390	1.389 (−1)	1.391 (1)
10,11	1.391	1.393 (2)	1.390 (−1)
11,12	1.389	1.388 (−1)	1.391 (2)
7,12	1.395	1.397 (2)	1.394 (−1)

[a] DFT/B3LYP/TZ2P values. Bond lengths in Å. [b] Numbers in parentheses are differences (in 10^{-3} Å) from the values for D = 25.6°.

The prediction that D is closer to 0 than to 90° can thus be attributed in significant part to pseudoconjugation. Other factors of particular importance in determining the equilibrium geometry of **1** can be further exposed by examining the variation in nonbonded distances as the value of D is varied. The changes in the distances O1···H17, O1···C12, H4···H13 and H5···H17 with D are shown in Figure 3 for the DFT/B3LYP/TZ2P calculations. At D = 0, O1···H17, O1···C12, H4···H13, and H15···H17 are 2.76, 3.01, 2.36, and 2.33 Å, respectively. We note that the O1···C12, H4···H13, and H5···H17 distances are less than the corresponding van der Waals distances (also indicated in Figure 3). As D is increased, in the direction of the equilibrium value, C12 and H17 initially move closer to O1, H4 moves further from H13, and H5 moves further from H17. O1···H17 and O1···C12 reach minimum values at D = 45° and then increase. The O···H distance is less than the van der Waals distance for D values in the range 20−70°. The H4···H13 and H5···H17 distances become greater than the van der Waals distance at D values <15° and continue to increase as D increases further. As D is increased from 0° in the direction away from the equilibrium geometry C12 and H17 initially move further from O1, H4 moves further from H13, while H5 moves closer to H17. H5···H17 decreases to a minimum at D = 25° and then increases. The minimum distance, 2.16 Å, is >0.2 Å less than the van der Waals distance.

The tilted conformation of **1** can be straightforwardly rationalized as the result of the balance between pseudoconjugation, attractive interaction of the ortho C−H group (C12−H17) with the oxirane O, and van der Waals repulsion of ortho H and oxirane H atoms H13/H4 and H17/H5. At the tilted conformation of **1** O1···C12 and O1···H17 are 2.906 and 2.546 Å, respectively, indicative of C−H···O H-bonding.[30] Phenyl rotation from D = 0° in the observed direction increases

(27) See, e.g.: Closs, G. L.; Klinger, H. B. *J. Am. Chem. Soc.* **1965**, *87*, 3265. Parr, W. J. E.; Schaefer, T. *J. Am. Chem. Soc.* **1977**, *99*, 1033 and references therein.

(28) de Boer, J. S. A. M.; Loopstra, B. O.; Stam, C. H. *Rec. Trav. Chim. Pays-Bas* **1987**, *106*, 537.

(29) Emsley, J. *The Elements*; OUP: New York, 1989.

(30) Desiraju, G. R. *Acc. Chem. Res.* **1991**, *24*, 290.

H-bonding to O, decreases H···H repulsion, while simultaneously decreasing pseudoconjugation. The balance occurs at a value of D between 0° and the value, 45°, minimizing the C−H···O distance and maximizing H-bonding. Phenyl rotation from D = 0° in the opposite direction causes pseudoconjugation to decrease, H-bonding to decrease, and H5···H17 repulsion to increase. The maximum energy occurs at a value of D between 90° and the value, 25°, minimizing the H5···H17 distance and maximizing H5···H17 repulsion. In sum, the variation in energy with D associated with the variation in pseudoconjugation is supplemented by attractive H-bonding and repulsive H···H van der Waals forces. These additional contributions significantly change the extrema of the PES on phenyl rotation both in energy and in angle.

Experimental values for the dipole moment of **1** in solution have been reported to be 1.82 ± 0.02 D in benzene[9] and 1.81 ± 0.02 D in CCl_4.[10] DFT/B3LYP/TZ2P and DFT/B3PW91/TZ2P values are 1.81 and 1.75 D, respectively. Corresponding 6-31G* values are 1.81 and 1.79 D. HF/SCF and MP2 6-31G* values are 2.08 and 2.26 D, respectively. The B3LYP values are the most accurate and agree with experiment within experimental error. The results support the superior accuracy of the DFT/B3LYP/TZ2P calculation and the reliability of the structure of **1** predicted at this level. In addition, since the dipole moment is calculated at a single conformation of **1**, our results reinforce the prior conclusion[10] that the observed dipole moment is inconsistent with free rotation of the phenyl ring, as proposed in the earliest dipole moment studies.[9]

While an X-ray structure of **1** has not been reported to date, structures do exist for substituted derivatives.[7,31] Of these, the *p*-nitro derivative (**2**) is the closest to **1**.[7] The reported structural parameters for **2** are given in Table 1. The conformation is tilted with a tilt angle of 9.8° and a dihedral angle D of 20°. In comparison to the DFT/B3LYP/TZ2P calculation for **1**: the C2−O1 and C3−O1 bond lengths differ by 0.000 and 0.001 Å, while C2−C3 differs by 0.026 Å; C3−C7 differs by 0.001 Å; phenyl C−C bond lengths differ by 0.006−0.014 Å, the largest differences being for C9−C10 (0.013 Å) and C10−C11 (0.014 Å). Bond angles differ by −2.1 to +0.7°. The torsional angles C8−C7−C3−H4, C1−C3−C7−C12, and C2−C3−C7−C12 differ by 5.6°, 7.6°, and 7.7°, respectively. Some part of these differences could be attributed to the nitro-substitution of the phenyl ring. To illuminate the magnitude of this contribution we have calculated the DFT/B3LYP/TZ2P geometry of **2**, with results also given in Table 1. The largest bond length change from **1** is 0.004 Å (C8−C9). The largest angle change is 2.2° (C9−C10−C11). The changes in the dihedral angles O1−C3−C7−C12, C2−C3−C7−C12, and C8−C7−C3−H4 are all <2°. Thus, the largest changes induced by *p*-nitro substitution are in bond lengths and angles close to the NO_2 group. The changes are much smaller in magnitude than the largest differences between the calculated structural parameters of **1** and the experimental parameters of **2**. It follows that these differences are either due to calculational error, to changes in the structure of **2** resulting from intermolecular interactions in the crystal, or to experimental error. We have discussed above the probable errors in the DFT/B3LYP/TZ2P structural parameters of **1**. The differences between calculated and experimental bond lengths for C2−C3, C9−C10, and C10−C11 are much greater than the calculational errors, dramatically so in the case of C2−C3. For these parameters, we conclude that intermolecular effects and/or experimental errors are substantial.

(31) See, e.g.: Merlino, S.; Lami, G.; Macchia, B.; Macchia, F.; Monti, L. *J. Org. Chem.* **1972**, *37*, 703.

The structure of **1** in solution was previously deduced from electrooptic Kerr effect measurements.[10] A tilt angle of 18 ± 9° was obtained. This result compares well with the DFT/B3LYP/TZ2P tilt angle of 14.5°.

Calculations of the tilt angle of **1** were previously reported using the CNDO/2 method. Values of ∼35[11] and ∼30°[12] were obtained, much larger than the ab initio values obtained here.

Our calculations have shown and the vibrational analysis has confirmed that **1** possesses a single conformation. According to the results shown in Figure 3, the barrier to internal rotational of the phenyl ring is 2.41 kcal/mol; the barrier occurs at D = 58°. There have been no experimental measurements of these parameters. CNDO/2 calculations (using rigid oxirane and phenyl geometries) predicted barriers of 3.54[11] and 3.15[12] at tilt angles of ∼35[11] and ∼30°.[12]

Conclusion

Increasingly accurate calculated PESs lead to increasingly accurate calculated vibrational frequencies and intensities. The relative accuracies of PESs calculated using different methodologies can therefore be gauged from the relative accuracies of predicted vibrational frequencies and intensities. Increasingly accurate PESs possess increasingly accurate equilibrium geometries. Thus, the more accurate predicted vibrational frequencies and intensities, the more accurate the predicted equilibrium geometry.

We have investigated the molecular structure of **1** in solution using vibrational unpolarized absorption and circular dichroism spectroscopies and ab initio theory. DFT calculations using hybrid functionals and the TZ2P basis set are in excellent agreement with experimental spectra. B3LYP gives better agreement than B3PW91. 6-31G* calculations are of somewhat lower accuracy. MP2/6-31G* and HF/SCF/6-31G* calculations are of much lower accuracy. As a result, it follows that the DFT/B3LYP/TZ2P geometry is the most accurate of the predicted geometries.

The DFT/B3LYP/TZ2P geometry is tilted by 14.5° from the bisected conformation in which the phenyl and oxirane rings are perpendicular. The tilt angle is intermediate between the value maximizing pseudoconjugation and the value maximizing hydrogen bonding of one phenyl ortho C−H to the oxirane O and can be rationalized in terms of these competing forces together with the contributions of nonbonding H···H repulsions. Evidence for pseudoconjugation is provided by the variation in C3−C7 on rotation of the phenyl group and by comparison of C2−C3, C3−O1, C7−C8, and C7−C12 bond lengths with corresponding bond lengths in oxirane and benzene.

Comparison of the predicted geometry of **1** with the solid-state structure of *p*-nitrophenyloxirane, obtained by X-ray crystallography, shows several substantial discrepancies, the most striking being in the C2−C3 bond length. The DFT/B3LYP/TZ2P C2−C3 bond length in **1** is 0.009 Å longer than the calculated C−C bond length in oxirane, which agrees with experiment within experimental error. The X-ray value of C2−C3 in **2** is 0.014−0.022 Å shorter than the experimental C−C bond length in oxirane. A DFT/B3LYP/TZ2P calculation for **2** does not resolve this discrepancy. Either rather large and specific solid-state interactions or error in the X-ray structure determination appear to be responsible.

Residual differences between the DFT/B3LYP/TZ2P calculations and experimental spectra can be attributed to (i) errors in the B3LYP functional, (ii) basis set error, (iii) anharmonicity, (iv) solvent effects. Calculations on small molecules lead to the conclusion that the differences between DFT/B3LYP/TZ2P

harmonic frequencies and gas-phase experimental frequencies are attributable predominantly to anharmonicity.[22] Given the very low dielectric constants of CCl_4 and CS_2, we expect solvent effects to be minor. The largest error in our results thus probably arises from the neglect of anharmonicity. Calculations including anharmonicity should be practicable soon and will be of interest. We note, however, that while the addition of anharmonic terms to the harmonic PES will improve the accuracy of predicted vibrational spectra, it will not change the equilibrium geometry.

In this work we have utilized unpolarized absorption and circular dichroism spectroscopies. The inclusion of VCD spectroscopy enables an analysis of the vibrational spectrum of **1** more definitive than obtainable from the unpolarized absorption spectrum alone. Additional study of the Raman and Raman optical activity (ROA) spectra of **1** would further test the conclusions of this work and is planned. (We note that experimental Raman and ROA spectra have already been reported.[32])

Acknowledgment. We are grateful to Professor L. A. Nafie, Dr. A. Rilling (Bomem Inc.), and Dr. R. Dukor (BioTools) for technical assistance with the Chiral*IR* spectrometer; to Drs. M.J. Frisch and J.R. Cheeseman for the GAUSSIAN 95 development code and for very helpful discussions; to NIH for support (R01, GM51972); and to the San Diego Supercomputer Center for computer time.

JA983302Y

(32) Hecht, L.; Barron, L. D. *J. Raman Spectrosc.* **1994**, *25*, 443; *J. Mol. Struct.* **1995**, *347*, 449.